Plant Chemistry/Biochemistry

pH-Dependent Lignin Cross-Linking Predominates Over Lignin Structure in Controlling Maize Cell Wall Degradability

J.H. Grabber, R.D. Hatfield, and J. Ralph

Introduction

The enzymatic degradation of fiber in grasses declines during plant maturation due to progressive lignification of primary and secondary cell walls. In most cases, lignified primary walls are less degradable than secondary walls. Differences in the rate of monolignol secretion into the apoplast and apoplastic pH during lignification may contribute to degradability differences between primary and secondary walls. Rapid "bulk" polymerization, as may occur in primary walls, favors C-C coupling of monolignols into a highly branched polymer. A branched structure may enhance entrapment of structural polysaccharides by lignin, restricting access of hydrolytic enzymes into primary walls. In contrast, slow "end-wise" polymerization, as may occur in secondary walls, favors β–*O*–4 coupling of monolignols into a relatively linear polymer. A linear lignin structure is thought to permit greater access of hydrolytic enzymes into secondary cell walls. Apoplastic pH also influences lignin structure by altering the reactions of quinone methide intermediates formed by β–*O*–4 coupling of monolignols. Acidic conditions (pH <5) favor the reaction quinone methide intermediates with water, uronic acids, or neutral sugars to form relatively linear lignins substituted with α-hydroxyl groups or cross-linked by α-ester and α-ether linkages to cell wall polysaccharides (Fig. 1). Less acidic conditions (pH >5) enhance the reaction of quinone methide intermediates with monolignol hydroxyl groups to form lignins with a highly branched structure. In this study, dehydrogenation polymer-cell wall (DHP-CW) complexes were formed by *in situ* polymerization of coniferyl alcohol into primary walls to evaluate the effect of monolignol polymerization rate and apoplastic pH on lignin formation and cell wall degradability.

Methods

Primary cell walls isolated from suspension cultures of corn (*Zea mays* L.) were suspended in pH 4 or 5.5 buffers and synthetically lignified by gradual "end-wise" or rapid "bulk" polymerization of coniferyl alcohol. During lignification, the activity of cell wall peroxidase was monitored with guaiacol. DHP-CWs were collected on glass-fiber filters and washed thoroughly with water followed by acetone to remove non-incorporated coniferyl alcohol. Degradability was estimated by incubating DHP-CWs with a cocktail of fungal enzymes with pectinase, hemicellulase, and cellulase activities. DHP-CWs and indigestible residues were hydrolyzed with H_2SO_4 to estimate Klason lignin. Enzyme and acid hydrolysates from DHP-CWs and indigestible residues were analyzed for uronic acids and neutral sugars. DHP-CW complexes were saponified with 2 M aq NaOH to release alkali-labile ferulate and diferulates for analysis by GC-FID. Monomeric lignin products released from DHP-CWs by thioacidolysis were identified by GC-MS and quantified by GC-FID.

Results and Discussion

Coniferyl alcohol was more efficiently incorporated into cell walls as end-wise polymers at pH 5.5 (93%) than as bulk polymers formed at either pH (59-68%). End-wise lignification was less efficient at pH 4 (48%) due to inactivation of cell wall peroxidase. Therefore, if lignification of primary walls begins as a bulk polymerization process, it must quickly transition to a more end-wise process if large quantities of wall-bound lignin are to be formed. Extensive lignification of grass cell walls under acidic conditions would also be unlikely unless the abundance or acid tolerance of wall peroxidases far exceeds that of our model system. Thioacidolysis of cell walls revealed that end-wise polymers had 1.8 to 2.6 fold more ether inter-unit linkages and 70% fewer end-groups than bulk polymers (Table 1). Low pH enhanced the formation of ether linkages, particularly for end-wise polymers. End-wise and bulk polymers depressed the enzymatic degradability of cell walls to the same degree, indicating that both types of lignin have similar interactions with structural polysaccharides. In contrast, lowering apoplastic pH from 5.5 to 4.0 during lignification reduced the degradability of cell walls by about 25% (Table 2). Low lignification pH depressed wall degradability only as cell walls become hydrophobic with at least 10% lignin. In another experiment, it was observed that low lignification pH depressed the degradability of DHP-CWs formed with coniferyl alcohol but not with coniferaldehyde (Table 3). Although coniferaldehyde undergoes similar types of coupling reactions as coniferyl alcohol, β–*O*–4 coupling of coniferaldehyde does not permit benzyl ester and ether cross-linking of matrix components *via* nucleophilic addition to quinone-methide intermediates. Cross-links of this type are most readily formed under hydrophobic and acidic lignification conditions; the same conditions that depressed the degradability of DHP-CWs formed with coniferyl alcohol. The release of major neutral sugars and uronic acids by hydrolytic enzymes were uniformly depressed by forming lignins at low pH (Table 4), suggesting that cross-linking *via* quinone methide intermediates involved all types of structural polysaccharides. After exhaustive enzymatic hydrolysis, degradability differences for each cell wall sugar were very small (*ca* 25 mg/g), suggesting that benzyl ester and ether cross-links were only slightly more abundant when walls lignified under acidic conditions. Future work will be directed at characterizing the types and abundance of benzyl ester and ether cross-links formed in DHP-CWs and in naturally lignified plant cell walls.

Conclusion

Overall, our results suggest that lignification pH influences lignin-matrix interactions, perhaps by altering the abundance of benzyl ester and ether cross-links formed *via* lignin quinone methide intermediates. Additional studies are, however, needed to clearly establish the existence of these cross-links in our model system and whether acidic conditions increase their abundance in cell walls. Our results suggest that small variations in benzyl ester and ether cross-linking can have a considerable impact on cell wall degradability. These results further support our contention that cell wall degradability is influenced by the amount of lignin in cell walls and its interactions with matrix components and not by normal variations in lignin composition or structure. The latter may only influence cell wall degradability if they markedly alter the hydrophobicity of lignin or its propensity to form cross-linked structures with other cell wall components.

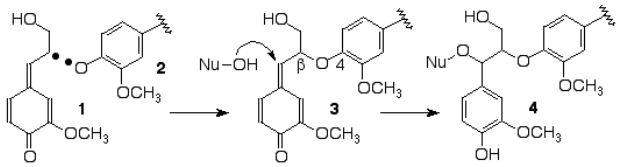

Figure 1. Monolignol **1** and lignin **2** radicals can undergo β-*O*-4 coupling to form quinone methide intermediates **3**. These intermediates are stabilized by the addition of nucleophiles (Nu), such as water, uronic acids, and neutral sugars to form structures **4** which are substituted with α-hydroxyl groups or cross-linked by α-ester and *α*-ether linkages.

Table 1. Klason and mass balance lignin concentrations (mg/g), and guaiacyl (G) units (μmol/g) released by thioacidolysis of DHP-CWs. Values in parentheses indicate percent of yield derived from end groups.

Treatment	Klason lignin	Mass lignin	G yield
Bulk polymerization			
pH 4.0	123.8	76.1	556 (28.8)
pH 5.5	126.4	81.6	537 (26.2)
End-wise polymerization			
pH 4.0	117.3	71.7	1441 (9.5)
pH 5.5	122.8	103.9	949 (8.3)

Table 2. Carbohydrate released (mg/g) from DHP-CWs at a Klason lignin content 123 mg/g after 6 and 72 h of hydrolysis by Celluclast and Viscozyme.

Treatment	6 h	72 h
Bulk polymerization		
pH 4.0	128	385
pH 5.5	172	473
End-wise polymerization		
pH 4.0	128	367
pH 5.5	181	487

Table 3. Carbohydrate released (mg/g) from DHP-CWs at a Klason lignin content of 120 mg/g after 6 and 72 h hydrolysis with Celluclast and Viscozyme.

Treatment	6 h	72 h
Coniferyl alcohol		
pH 4.0	169	504
pH 5.5	259	520
Coniferaldehyde		
pH 4.0	155	395
pH 5.5	161	377

Table 4. Concentrations (mg/g) of arabinose (Arab), galactose (Gal), glucose (Glu), xylose (Xyl), and uronosyls (Uro) in DHP-CWs and their release (%) by fungal enzymes. DHP-CWs were lignified at pH 4.0 or 5.5 to a Klason lignin concentration of 123 mg/g.

	Arab	Gal	Glu	Xyl	Uro
Monosaccharide concentration					
DHP-CW	167.8	74.4	287.4	136.9	91.0
Release of monosaccharides					
6 h hydrolysis					
pH 4.0	19.8	19.1	19.0	10.5	26.5
pH 5.5	23.2	22.6	26.5	15.1	35.3
72 h hydrolysis					
pH 4.0	58.1	58.5	51.6	36.1	80.3
pH 5.5	71.8	73.8	66.1	50.0	82.9
Exhaustive hydrolysis					
pH 4.0	76.2	83.6	87.3	61.1	91.6
pH 5.5	79.6	85.8	90.7	63.6	93.3

A Comparison of Methods For Determining Lignin in Plant Samples

R Fukushima and R.D. Hatfield

Introduction

As forages mature there is generally a decline in digestibility of the fiber fraction (cell wall) that is associated with an increase in lignin. People have tried to use lignin concentration as a means of predicting cell wall and whole plant digestibility. This seems to work reasonably well as long as one is making comparisons within the same plant species. One of the problems when trying to compare published data from a range of plants is the type of lignin assay method used may vary. Not all procedures give you the same results. It has been shown that acid detergent lignin (ADL) methods result in a significant solubilization of lignin from grass cell walls, this is not the case with legumes or other plant samples. We have been interested in refining the acetyl bromide soluble lignin (ABSL) as a method for measuring lignin in forage samples. It is convenient and allows several samples to be run in a single day. It is also applicable to using small sample sizes if tissue size is a problem. We have compared a number of plant samples using the four most popular lignin methods, ADL, ABSL, permanganate lignin (PerL), and Klason lignin (KL). In addition, we have determined the IVDMD and IVCWD of these samples to see how the lignin values generated by these procedures correlate to digestibility.

Methods

Lignin standards for the acetyl bromide method were extracted from the cell walls of a wide range of plants (see Table 1 for a complete list). These same plants were used for the ABSL, ADL, PerL, and KL lignin determinations as well as materials for IVDMD and IVCWD determinations. All analyses were run in duplicate. Statisitical anlaysis was used to correlate lignin method concentration with digestibility characteristics.

Results and Discussion

In order to utilize the ABSL method, extinction coefficients for each type of isolated lignin were generated. Theoretically all lignin should give the same or similar results. As can be seen in Table 1 this is generally true with a couple of exceptions. Even though extraction of lignin from plant cell walls provides a relatively clean preparation of lignin it is still contaminated with small amounts (10-15%) of carbohydrates and proteins. Corrections for these contaminates is dependent upon accurate assessment of what and how much is in the different lignins in order to make adjustments for absolute weights of lignin.

Other methods of lignin determination also have a problem when it comes to determining the absolute amount of lignin. As already mentioned the ADL method can greatly underestimate the total lignin in forage samples, especially grasses. This is due to the partial solubility of lignin/lignin-carbohydrate complexes in the hot detergent solution. This is not as much of a problem for legumes suggesting that the lignin structure of these two different types of plants differs in their physio chemical make up. Permanganate lignins are based upon the ability to oxidize the lignin from a plant cell wall without affecting the cell wall carbohydrates. This method was developed originally for woody species in which the cell wall carbohydrate was predominately cellulose. In forages the cell wall contains significant amounts of other polysaccharides that are quite susceptible to oxidation by

permanganate. For non-woody species this procedure tends to give much more variable results depending upon the cell wall make-up. Klason lignin is one of the oldest procedures and is frequently used for forage samples. The ADL procedure is basically the same except for the hot acid detergent treatment to insure the removal of protein and non-cellulosic polysaccharides before acid solubilization of cellulose. Klason lignin values tend to be over-inflated due to the potential for protein contamination. This is not too much of a problem with samples that are typically low in protein such as stem tissues. The acetyl bromide method does not have the problems of contaminating materials since it is based on absorbance of lignin dissolved in the reaction mixture. However, it is important to start with a sample preparation in which small molecules (simple phenolics compounds) have been removed, i.e., doing cell wall isolation before analysis. Also carbohydrate degradation during the heating step can contribute to some additional non-lignin absorbance.

We have compared several forage samples using these four lignin techniques to determine how each procedure within general groupings of plant samples (Table 2). From the data in Table 2 it is clear that each procedure generates a different lignin value. Depending upon the sample type some procedures given similar results; for example generally Klason lignin and ABSL procedures generated numbers that were similar across all species. It is not possible to say that one type of method gives the true lignin value for a given forage species. We also compared the digestibility of these forage materials (Table 2). Statistical correlation analysis of the lignin data with digestibility data indicated that no method was highly correlated to digestibility, although Klason and ABSL provided the best correlations (Table 3).

Conclusions

It would appear that the acetyl bromide method for determining lignin concentration holds promise as a technique for quickly estimating digestibility in a wide range of plants. Further work with a wider range of forage plants, maturities, and environmental growing conditions is needed in order to determine if this relationship will hold up or be improved

Table 1. Lignin coefficients developed for the acetyl bromide lignin method based on lignins isolated from each type of plant material.

Plant Material Description	MEAN	
Alfalfa FB lower 30	14.23	
Alfalfa FB upper 30	15.99	
Alfalfa PSD	15.30	
Alfalfa Y	15.69	
Bromegrass M1	17.11	
Bromegrass M2	16.73	
Bromegrass M3W	17.40	
Bromegrass Y	17.44	
Cornstalk PA	17.75	
Oat straw leaf	20.10	
Oat straw stem	18.91	
Red clover FB	14.49	
Wheat straw leaf	19.81	
Wheat straw stem	17.54	Overall Mean 17.04 ± 1.80

FB= full bloom, PSD= seed development, Y=young, pre bud stage, M1=pre-boot stage, M2= anthesis, M3W= post anthesis, PA= post anthesis

Table 2. A comparison of lignin values generated from application of the four different lignin methods. All values are given in mg g^{-1} cell wall. Also the in vitro dry matter digestibility (IVDMD) and the in vitro cell wall digestibility (IVCWD) is given for each sample.

	mg g^{-1}											
Plant Material	ADL		KL		PerL		ABSL		IVDMD		IVCWD	
	Avg	± STDev	avg	± STDev	avg	± STDev	avg	± STDev	avg	± STDev	avg	± STDev
Alfalfa FB lower30	92.5	±3.0	144.8	±0.4	157.6	±16.8	134.7	±1.6	418.4	±21.3	240.6	±27.7
Alfalfa FB upper 30	59.3	±0.3	111.4	±0.6	95.3	±10.9	71.4	±4.9	616.6	±37.5	394.9	±6.6
Alfalfa PSD	90.6	±1.4	138.8	±1.0	153.8	±10.5	117.3	±2.3	443.2	±11.4	254.1	±13.8
Alfalfa Y	83.6	±2.0	123.0	±3.1	134.7	±6.7	116.6	±4.3	438.1	± 8.8	320.9	±7.7
Bromegrass M1	30.4	±0.1	100.4	±13.8	64.1	±1.7	127.5	±0.4	451.6	±12.8	298.1	±5.9
Bromegrass M2	36.5	±1.3	109.8	±15.6	69.9	±6.4	144.6	±12.9	401.0	±20.4	252.8	±14.1
Bromegrass M3W	45.6	±1.7	130.1	±0.1	67.1	±1.1	139.1	±5.2	366.3	±18.6	139.9	±10.3
Bromegrass Y	28.5	±1.5	102.2	±5.8	56.0	±0.7	123.4	±0.2	527.2	±24.0	365.1	±21.7
Corn stalk PA	24.8	±0.2	76.7	±7.8	45.2	±13.2	92.0	±2.9	498.2	±0.0	289.4	±7.8
Oat straw leaf	106.9	±2.8	138.1	±1.9	71.3	±8.1	123.5	±0.3	254.5	±10.9	331.0	±22.3
Oat straw stem	83.3	±0.6	171.2	±1.6	111.5	±5.4	186.3	±5.9	124.6	±25.0	92.9	±16.9
Red clover FB	41.7	±1.3	71.3	±1.5	115.6	±8.1	90.4	±1.1	531.0	±10.6	410.5	±28.8
Wheat straw leaf	103.4	±10.5	141.6	±0.1	74.3	±11.6	149.9	±3.4	233.8	±26.6	336.5	±22.3
Wheat straw stem	89.1	±10.8	184.2	±2.1	122.0	±12.9	213.0	±15.0	129.7	±58.6	61.6	±22.2

ADL= acid detergent lignin, KL= Klason lignin, PerL=Permanganate lignin, ABSL= acetyl bromide soluble lignin

Table 3. Correlation analysis of lignin determination method with digestibility.

Digestibiltiy	ADL	KL	PerL	ABSL
IVDMD	-0.44	-0.64	-0.06	-0.76
IVCWD	-0.23	0.74	-0.21	-0.83

Characteristics of Red Clover Polyphenol Oxidase

R.D. Hatfield, K. Frost, and M.L. Sullivan

Introduction

Polyphenol oxidase (PPO) also known as O-diphenol oxidase and catechol oxidase, is widely distributed among higher plants. In the presence of oxygen, PPO catalyzes the oxidation of *o*-diphenols to *o*-quinones which non-enzymatically polymerize with proteins and other phenols to produce brown pigments. This property makes the PPO enzyme an important enzyme in the food industry because it often causes post-harvest browning of fruit and vegetable crops leading to off flavors and loss of nutritional quality. To date, no clear function of PPO has been established within the plant, but the characteristic browning of fruit and vegetable tissues and extracts such as banana, grape, blueberry, sweet potato, and loquat have been studied. The distinctive browning reaction of PPO has also been observed in the forage legume red clover (*Trifolium pratense*). However, unlike many of the fruit and vegetable crops, the browning reaction in red clover has been correlated to a reduction of proteolysis in the silo, a desired outcome for producers. The mechanism for this reduction of proteolysis is still unknown, but it is thought to involve both the PPO enzyme and its substrates. We have been characterizing the chemical and biochemical properties of the red clover PPO enzyme in order to possibly determine its function in the plant as well as to understand the mechanism for the reduced proteolysis in red clover silage.

Methods

Fresh red clover leaves were ground to a fine powder under liquid nitrogen before extraction with 20 mM TRIS buffer (100 mM sodium acetate, 50 mM sodium ascorbate, 5% glycerol, pH 7.9). Partially purified PPO extracts were analyzed to determine the pH optimum, temperature optimum, molecular weight, and substrate specificity. A spectrophotometric assay using 5-thio(2-nitrobenzoate) (TNB) as a chromophore was used to monitor PPO activity. The substrate, caffeic acid, when oxidized by PPO to an *o*-quinone reacts with the sulfhydryl group on TNB forming a caffeoyl sulfhydryl conjugate that has decreased absorbance at 412 nm. The assay solution consisted of 20 μl of 100 mM caffeic acid (dissolved in 95% ethanol), 20 μl of TNB solution, 950 μL of 20 mM TRIS buffer (pH 7.0) and 10 μL of the enzyme solution. One unit of activity was defined as the amount of enzyme that resulted in decreased absorbance of 1 unit min^{-1}. For substrate specificity determinations various *o*-diphenols were substituted for the caffeic acid. A 0.01 M piperazine hexahydrate and 0.01 M gly-gly buffer with pH ranging from 4.5 to 9.0 was used to determine the optimal pH for PPO activity. For temperature optimum 20 mM TRIS buffer (pH 7.0) containing caffeic acid (0.25 mM) was used to measure PPO activity directly by monitoring the absorbance shift of caffeic acid (284 nm) as it reacts with the PPO. Absorbance change was monitored for 5 minutes over a range of temperatures from 10-70 ˚C. Temperature stability was measured under the same conditions except that the PPO enzyme solution was pre-incubated at various temperatures for 1, 2, and 4h prior to adding to the reaction mixture.

Results and Discussion

The red clover PPO was partially purified utilizing a series of chromatographic steps including two size exclusion columns Toyopearl HW-40 and Toyopearl HW-55 followed by anion exchange chromatography Toyopearl 650-DEAE. One of the problems with the red clover system is that there

is such a high level of soluble phenolics (including the *o*-diphenol substrates for PPO) that enzyme activity is quickly lost if the enzyme is not separated from these materials. On a small scale (1-3 mL) this can be accomplished quite rapidly and produce a stable crude extract. Increasing the size of the extract results in a significant loss of total activity; however sufficient amounts were obtained that allowed further purification and characterization of the PPO. We were able to obtain an approximately 1400-fold increase in specific PPO activity reflecting a significant amount of enzyme purification. This resulted in an approximate 4% recovery of total protein from the original extract.

The properties of red clover PPO were similar to those published from other species and are summarized in Table 1. The one interesting observation concerning the PPO properties is the maintenance of good PPO activity (≥ 50%) over a wide range of pH conditions. This would probably aid in the effectiveness of inhibiting proteolytic activity in red clover silage since it would be able to maintain good activity as the pH is dropping and the limitation would only be the availability of oxygen required to produce the *o*-quinones. This may help explain why red clover produces good silage even though the pH has not dropped to a level typically thought to be important to inhibit proteolytic activity.

Of particular interest in characterizing red clover PPO is to determine the effectiveness in utilizing a range of *o*-diphenol substrates. There are two *o*-diphenol compounds that have been identified in red clover, phasic acid and clovamide (Fig. 1). We have not been successful in purifying sufficient amounts of these compounds for in vitro chemical analyses. However, we have been able to monitor both compounds in crude extracts of red clover as the endogenous PPO utilizes them. Phasic acid and clovamide are both rapidly utilized in the crude extracts. Since both are derivatives of caffeic acid (Fig. 1) we investigated a range of other *o*-diphenols to determine the effectiveness as PPO substrates (Table 2). From these results it is clear that caffeic acid and close derivatives of it are the preferred substrates of the red clover PPO.

Conclusions

Red clover polyphenol oxidase is a soluble enzyme with an apparent molecular weight of 68 kD. It has relative good temperature stability and is active over a fairly wide pH range (4.5-8.0). These are important characteristics that may contribute to the sustained activity during the ensiling process for red clover. Red clover PPO can utilize several *o*-dihenols, but has much higher activity with substrates that are caffeic acid derivatives.

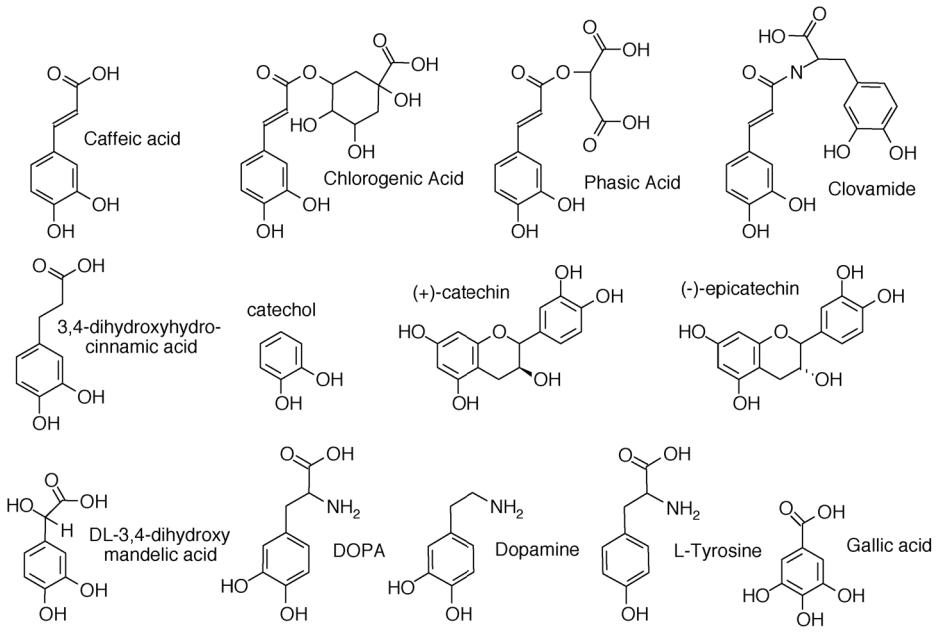

Figure 1. Structural characteristics of O-diphemols tested as possible substrates for the red clover PPO.

Table 1: Properties of the PPO enzyme extracted and partially purified from red clover. All enzyme activities are based upon caffeic acid as the *o*-diphenol substrate.

PPO Characteristic	Value	Comments
Molecular weight	68kD	Based on SDS-PAGE
	71kD	Based upon gel filtration chromatography
pH optimum	6.5-7.0	50% activity fro 4.5 to 8.0 pH
Temperature optimum	25 °C	Broad range 80% activity from 15-35°C
Temperature stability	50 °C	Based on 2h preincubation

Table 2. Relative activities of *o*-dipenol substrates utilized by red clover polyphenol oxidase

Substrate	Relative Activity
caffeic acid	100
phasic acid (estimated)	+90
clovamide (estimated)	+90
chlorogenic acid	96
3,4-dihydroxyhhydrocinnamic acid	28
catechol	24
(-) epicatechin	7
(+) catechin	6
dopamine	6
L-DOPA	3
gallic acid	2
DL-3,4-dihydroxymandelic acid	1
protocatechuic acid	1
tyrosine	0

Non-degradative Dissolution and Acetylation of Ball-milled Plant Cell Walls; High-resolution Solution-state NMR

F. Lu and J. Ralph

Introduction

The ability to dissolve plant cell walls without degradation would provide significantly improved methods for cell wall structural analysis and allow standard solution-state derivatization and reaction chemistries to be more effectively applied.

Researchers have therefore been anxious to develop methods that might allow the entire lignin fraction, and indeed the whole cell wall, to be analyzed by NMR. In the past, we and others have tried to apply the various cellulose solvent systems to the whole cell wall, but with little success. Other dissolution methods are simply too destructive on the components of the wall. Here we describe a solvent system (one of two that we have developed) that fully dissolves finely divided (vibratory ball-milled) cell walls, apparently non-degradatively. Ball-milling is commonly used in lignin isolation procedures. *In situ* acetylation is demonstrated for its value in providing derivatized cell walls that are completely soluble in chloroform. The derivatized cell wall can therefore be analyzed by high-resolution solution-state NMR methods, providing considerable insight into wall structure without the need for polymer fractionation. This work is all on wood cell walls; we make no apologies for developing techniques on the cleaner and more readily available woods first since if it does not work for wood, it won't work for anything. We shall of course be developing these methods for forages in the near future.

Results and Discussion

Cell wall dissolution in DMSO-NMI

A system not previously described as a cell wall or even a cellulose solvent system has the properties required to produce cell wall materials in a form suitable for NMR; it rapidly and completely dissolves the wall, allows for facile derivatization reactions such as acetylation, and can be used to generate products ideal for solution-state NMR. The system is N-methylimidazole in DMSO (DMSO/NMI). Complete dissolution of a variety of ball-milled cell wall materials can be effected in 1-3 h at room temperature. The solutions are homogeneous and clear. N-methylimidazole is an excellent acylation catalyst, so *in situ* acetylation (for example) is readily accomplished. The acetylated cell wall (Ac-CW) is readily isolated, essentially quantitatively, by precipitating into water. It is completely soluble in chloroform or methylene chloride.

NMR of Acetylated Cell Walls

Fig. 1 shows a picture of NMR tubes of Ac-CWs from pine and aspen woods, ca. 150 mg/mL in deuterochloroform ($CDCl_3$); the clarity of the solutions is demonstrated by the background (part of a plotted proton NMR spectrum) showing through the tubes. The solutions are rather viscous at over about 200 mg/mL, but quite mobile at <150 mg/mL. Such concentrations are quite suitable for NMR. However, the lignin component of interest, typically only ~20% of the cell wall, is now considerably more dilute than in samples of comparable total concentration prepared directly from isolated lignins. The 5-fold sensitivity decrease can be offset by utilizing higher-field instruments and/or cryogenically cooled probes.

Although the spectra were expected to be dominated by polysaccharide peaks, the various (acetylated) cellulose, hemicelluloses, and lignin resonances are well dispersed in 2D NMR, allowing substantive interpretation. Here we concentrate on the lignin assignments. Fig. 2 shows 1-bond ^{13}C–^{1}H correlation spectra taken on a 360 MHz spectrometer. The upper plots (a) show the lignin sidechain regions of the Ac-CW spectra and, for comparison and aid in spectral assignment, the same regions from spectra of isolated lignins from similar (but not identical) samples are shown in the lower plots (b).

As seen by the color coding in Fig. 2b1, the diagnostic lignin methoxyl, major β-ether units **A**, substantial phenylcoumaran units **B**, and more minor resinol **C** and dibenzodioxocin **D** units are well resolved in the guaiacyl acetylated milled-wood lignin (Ac-MWL) from pine. The predominantly guaiacyl (4-hydroxy-3-methoxyphenyl) lignins in pine (and softwoods in general) derive from the mono-methoxylated monomer coniferyl (4-hydroxy-3-methoxycinnamyl) alcohol. At least some of the sidechain correlations for all of these structures are also remarkably well resolved in the pine Ac-CW spectrum, Fig. 2a1.

Hardwood lignins, including the poplar lignin shown on the right of Fig. 2, derive more substantially from sinapyl (3,5-dimethoxy-4-hydroxycinnamyl) alcohol and have syringyl/guaiacyl lignins. The additional methoxyl at the aromatic ring 5-position precludes the involvement of syringyl units in 5-linked structures such as the phenylcoumaran **B** and the 5–5-linked moiety of dibenzodioxocins **D**. The lignins are characterized by a higher β-ether **A** content, as well as having more prominent β–β-coupled (resinol) units **C**. Also, cinnamyl alcohol endgroups **X** may be more prominent. The poplar Ac-MWL shows the prominent **A**, and **C** units, and minor amounts of **B** and **X**, Fig. 2b2. Again, these structures and the methoxyl are revealed in the related Aspen Ac-CW spectrum, Fig.

2a2 (although viewing at lower contour levels are needed to clearly see the **B** and **X** units).

The aromatic regions (not shown) are particularly noteworthy in that the aromatic components appear to be entirely due to the lignins as seen by the comparison of the aromatic profile between the Ac-CW and Ac-MWL spectra. Also the anomeric C/H regions for the polysaccharide components are extremely well resolved suggesting that substantive interpretation of these components will be possible. Reduced polysaccharide degree of polymerization (DP) caused by ball-milling is strongly evident. Cursory integration of the cellulose internal anomeric peak to the presumed acetylated α- and β-anomers of the reducing end units (at 88.9/6.22 and 91.5/5.63 ppm) suggest molar ratios of only 20-25:1. This DP estimate of 20-25 is considerably lower than the DP of cellulose reported *in planta*, in the 7-10,000 range, suggesting that ball-milling has cleaved the long cellulose chains hundreds of times. There is no evidence to suggest that the depolymerization is coming from the dissolution processes, but the findings heighten the need to evaluate less severe milling conditions for future work. There are a great variety of ball-milling methods. The steel ball-mill used here is extremely efficient, requiring only 1.5 h. for effecting particle-size reduction. Others use much longer times, and have strongly recommended ball-milling in toluene to avoid lignin structural alteration.

Fig. 3a further illustrates the value of being able to apply solution-state NMR methods. The 2D section is from the same aspen HSQC experiment used in Fig. 2c2, but plotted at much higher contour levels so that only the most intense peaks, essentially just the cellulose and methoxy contours, are seen. The spectrum at this level is almost identical for the pine Ac-CW (not shown). A short 1D ^{13}C experiment is shown on the left projection, with the 1D ^{1}H experiment on the top. Although there is some overlap of the carbons (notably carbons 5 and 3) and the protons (notably proton-1 and one of the 6-protons, as well as the lignin methoxyl with proton-4) in their respective 1D spectra (projections), all six carbon/proton pairs are beautifully resolved in the 2D experiment allowing all of the data to be readily determined. Also shown is a solid-state ^{13}C spectrum of pine wood, Fig. 3b. Although chemical shift comparisons are not valid for this sample compared to the acetylated cell wall in the remainder of the figure, the spectrum is included for comparison of linewidths and resolution. The solid-state spectrum provides additional information regarding the two allomorphic forms of crystalline cellulose, but the greater carbon linewidths (and the extreme linewidths of proton NMR data in solid-state spectra) preclude the acquisition of informative 2D spectra.

Obviously the Ac-CW material can be subjected to the whole range of solution-state NMR methods, including homonuclear correlation experiments such as COSY and TOCSY, and heteronuclear experiments such as the HSQC illustrated in Figs. 2 and 3, and also long-range ^{13}C–^{1}H correlation experiments. Even 3D experiments are perfectly viable, and should provide a way to obtain complete sidechain data for the individual lignin units since each unit is likely to be reasonably well isolated onto its own plane in a 3D TOCSY-HSQC experiment, for example.

Conclusions

Although a total interpretation of all the contours in the congested regions of the spectra is unlikely, it should be obvious that high-resolution solution-state NMR of (acetylated) whole cell wall material will be extremely valuable in assessing the structural components of the wall. The dispersion is sufficient that most lignin structures can readily be identified, and will be potentially quantifiable by

more quantitative versions of HMQC or HSQC spectroscopy. The degree of detail discernable is far higher than can be accomplished by solid-state NMR on solid material, and yet there is every indication that we are looking at the whole cell wall (that has admittedly been degraded by the ball-milling step). Sensitivity reduction caused by utilizing whole cell walls instead of isolated fractions can be largely offset by using cryogenically cooled probes that are becoming common in modern NMR instruments.

For the many valuable samples accumulated from previous studies of lignin-biosynthetic-pathway mutants and transgenics, we shall be applying these new methods to both the whole cell walls and to the residues remaining following the dioxane-water extraction of "milled wood lignins" from polysaccharidases-treated walls — often this material still contains the bulk of the lignin. It should be possible to observe the diagnostic signatures of gene-downregulation that have to date been noted only on the soluble component. For example, COMT-deficient angiosperms (poplar, aspen, corn, arabidopsis, and alfalfa) have been shown to incorporate substantial amounts of the novel monolignol 5-hydroxyconiferyl alcohol into their lignins when the pathway to sinapyl alcohol is down-regulated; this incorporation produces benzodioxane structures in the lignins. The diagnostic α- and β-C/H correlations appear at ~77/5.0 and 76/4.4 ppm, clear regions in the spectra in Fig. 2, suggesting that their detection will be straightforward.

A significant limitation at present is the need to finely grind the material. Fine-grinding, by a method such as vibratory ball-milling, that is already required to isolate lignin fractions, does of course break bonds and therefore reduces polymer DP (as shown here with the cellulose component) and causes structural alteration. We are assessing just how much milling is required. Cryogenic milling to a less fine state also appears to provide material that can be fully dissolved, although material mechanically ground to pass through a 1 mm mesh in a mechanical Wiley mill will not. Although we shall endeavor to find methods that work for less finely ground material, it is already extraordinarily useful to be able to prepare samples of the whole cell wall (and particularly the entire lignin component), without fractionation or partitioning the polymers, in days instead of weeks, for analysis by high-resolution solution-state NMR.

In conclusion, the ability to fully dissolve ball-milled plant cell walls, without further apparent degradation, portends enormous potential for applying high-resolution solution-state NMR to elucidate structural details without having to resort to the laborious isolation methods of the past. It is also expected that the systems will allow the application of standard chemical derivatization and reaction methods, significantly improving the old heterogeneous methods.

Experimental Procedures

Dissolution and Derivatization in DMSO/NMI

The ball-milled cell wall sample (600 mg) was suspended in DMSO (10 mL) and NMI (5 mL) was added. A clear solution formed in 3 h or less, depending on the sample.

Excess acetic anhydride (3 mL) was added and the mixture stirred for 1.5 h. The clear brown solution was transferred into water (2000 mL) and the mixture allowed to stand overnight. The precipitate was recovered by filtration through a nylon membrane (0.2 μm). The product was washed with water (250 mL) and dried under vacuum at room temperature. The weight of acetylated cell walls was typically 137-140% of the weight of the original cell wall.

[Color Figures that are more easily interpretable will be in the pdf version of these Research Summaries available from our web site. The full version of a paper on this subject will be available in the "Full Text Publications" section, directly at: http://www.dfrc.ars.usda.gov/DFRCWebPDFs/pdfIndex.html]

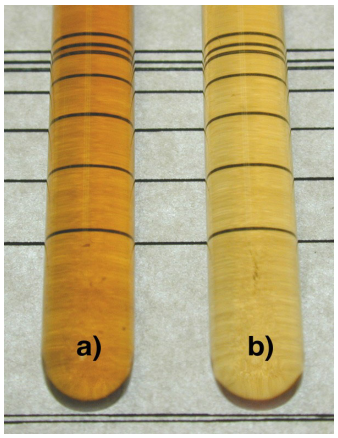

Figure 1. Plant cell walls can be solubilized for NMR. The picture shows NMR tubes containing solutions of acetylated CWs from solvent-extracted ball-milled a) pine wood and b) aspen wood from the DMSO/NMI system. Over 100 mg are dissolved in $CDCl_3$ (0.5 mL) in 5 mm tubes. The homogeneous solutions are viscous, but clear, as evident from the transmitted lines (from a paper-plot placed behind the tubes).

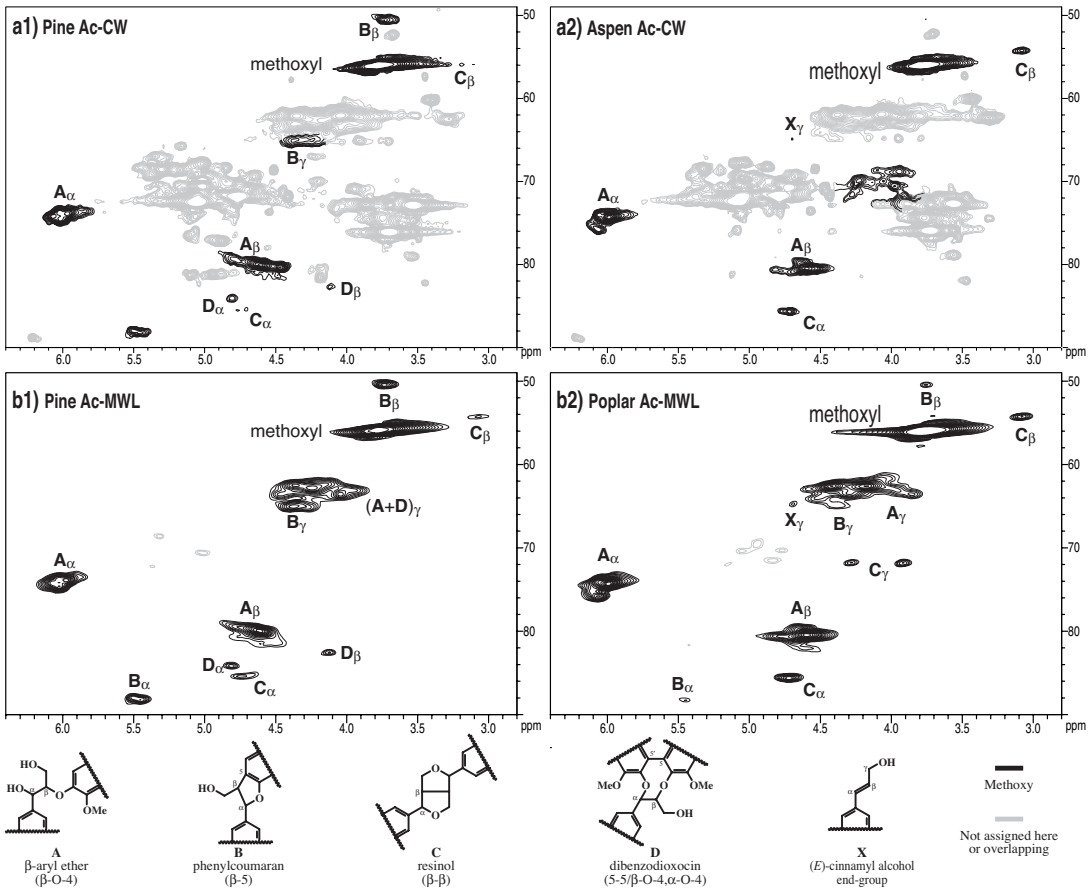

Figure 2. 2D HSQC NMR spectra of acetylated cell walls and isolated lignins. Spectra from samples in $CDCL_3$ show how readily the lignin components can be seen even in complex whole cell wall mixtures of pine (left column, 1) and aspen/poplar (right column, 2). a-b) zoomed-in lignin sidechain region. Note how well resolved at least one correlation is for each major lignin structure. The predominant lignin structures **A**-**D**, **X**, and the methoxyl are highlighted, in CW samples (Figs. a) where they can be clearly defined.

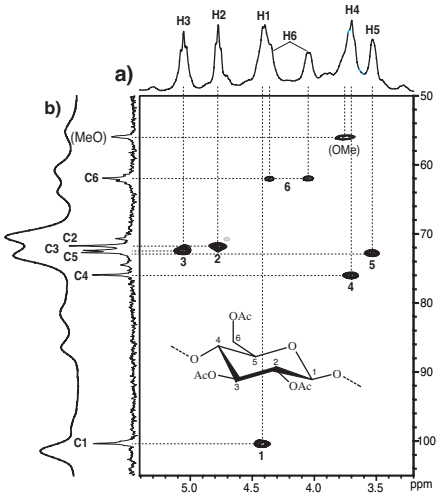

Figure 3. The cellulose component. a) The cellulose (and methoxyl) region of the 2D HSQC spectrum of aspen Ac-CW showing the advantage of solution-state NMR in completely resolving all C/H correlations. b) A solid-state NMR spectrum of pine wood simply for comparison of line widths.

Synthesis of Hydroxycinnamoyl-L-Malic Acids and Identification of 5-Hydroxyferuloyl-L-Malic Acid in COMT-Downregulated *Arabidopsis*.

P. Schatz, C. Lapierre, and J. Ralph.

Introduction

Hydroxycinnamoyl-L-malic acids are natural products that have been isolated from a variety of plants, e.g., sinapoyl-L-malic acid **1a** from red turnip (*Brassica campestris* L.*)* and *Arabidopsis*, phaselic acid **1c** from kidney beans (*Phaseolus vulgaris*) and red clover (*Trifolium pratense*), and *p*-coumaroyl-L-malic acid **1d** and feruloyl-L-malic acid **1e** from radish (*Raphanus sativus*). Our interest in this type of compound has been piqued by the severe reduction in sinapoyl malate **1a** in plants which have been downregulated in a crucial lignin-biosynthetic-pathway enzyme, COMT. Interestingly, when COMT is downregulated in *Arabidopsis*, the novel 5-hydroxyferuloyl-L-malic acid **1b** is observed, paralleling the incorporation of the novel monolignol 5-hydroxyconiferyl alcohol into its lignins.

Since the structural assignments of **1a** and **1b** were based on mass spectral data only, we sought to confirm the assignments by synthesis of the authentic compounds. To date, the only reported synthesis of a cinnamoyl-L-malic acid is the synthesis of phaselic acid **1c** by Scarpati and Oriente. This approach was not amenable for the target molecules.

Methods and Materials

The *t*-butyl ester of L-malic acid **3c** was prepared by a circuitous, yet necessary, route involving protection of the hydroxyl group on malic acid **2**, Fig. 2. L-Malic acid **2** was heated with excess acetyl chloride to yield the acetate anhydride. This was hydrolyzed to 2-acetoxy-L-malic acid **3a** by

stirring overnight with water. The *t*-butyl ester of 2-acetoxy-L-malic acid **3b** was prepared by acid catalyzed addition of isobutylene. Hydrolysis of the acetate group was carried out with aqueous sodium hydroxide to afford di-*t*-butyl L-malate **3c**.

The required substituted cinnamoyl chlorides were prepared starting with appropriately substituted aldehydes, syringaldehyde **4a** and 3,4-dihydroxy-5-methoxybenzaldehyde **4b**. The hydroxyl groups were protected by converting them to acetates **4c** and **4d** using pyridine and acetic anhydride.

The α,β-unsaturated esters, **5a** and **5b**, were prepared from the protected aldehydes using the Wadsworth-Emmons modification of the Wittig reaction (*tert*-butyldiethylphosphonoacetate and NaH as the strong base). Hydrolysis of the *t*-butyl esters with 90% trifluoroacetic acid afforded the acids **5c** and **5d**, which were subsequently converted to the acid chlorides **5e** and **5f** using thionyl chloride.

Coupling of the acid chlorides with di-*t*-butyl L-malate **3c** yielded esters **6a** and **6b**. The acetate groups were removed using pyrrolidine to afford **6c** and **6d**. Finally, the *t*-butyl groups were removed using 90% trifluoroacetic acid to yield sinapoyl-L-malic acid **1a** and 5-hydroxyferuloyl-L-malic acid **1b.**

Results and Discussions

We preferred a synthetic approach which did not require chromatography nor require a Craig apparatus to isolate the product. In the method developed, the acid groups of malic acid were masked as *t*-butyl esters which were hydrolyzed in the last step of the synthesis. Since the hydrophilic groups (hydroxyls and acids) were masked, isolation and purification of the intermediate products was greatly simplified. In the last step, hydrolysis conditions can be controlled to minimize the presence of water and thus facilitate isolation of the very water-soluble final products.

The synthesized sinapoyl malate **1a** and 5-hydroxyferuloyl malate **1b** were found to be the same products as those produced in wild-type and COMT-deficient arabidopsis. COMT is the enzyme that methylates 5-hydroxyconiferaldehyde to sinapaldehyde which is reduced to the monolignol sinapyl alcohol in the monolignol biosynthetic pathway. It has now been well established that COMT-deficient plants utilize a product of incomplete monolignol biosynthesis, 5-hydroxyconiferyl alcohol, as a substitute monomer for sinapyl alcohol for their lignification, producing novel benzodioxane structures in the lignin polymer.

The sinapoyl ester pool is also affected by COMT-downregulation. It seems logical that plants are effectively utilizing 5-hydroxyconiferyl alcohol to make a functional lignin polymer, and these products suggest that other biochemical pathways (e.g. to sinapoyl malate) also have the flexibility to accommodate the substitution of 5-hydroxyferuloyl analogs (although the specificity of the enzymes involved is unknown). Whether the plant is “deliberately” making these sinapate analogs as functional alternatives, or whether they are simply unanticipated products resulting from sloppy transferase enzyme specificity become intriguing issues to ponder for future research. The COMT-deficient Arabidopsis plants are not noticeably more susceptible to UV exposure (sinapoyl malate is a major UV-protecting agent in Arabidopsis) suggesting that the plant is “deliberately” utilizing the 5-hydroxy analog in a similar role.

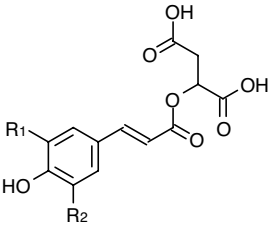

1a $R_1 = R_2 =$ OMe (sinapoyl malate)
1b R_1 = OMe, R_2 = OH (5-hydroxyferuloyl malate)
1c R_1 = OH, R_2 = H (phaselic acid)
1d $R_1 = R_2 =$ H (*p*-coumaroyl malate)
1e R_1 = OMe, R_2 = H (feruloyl malate)

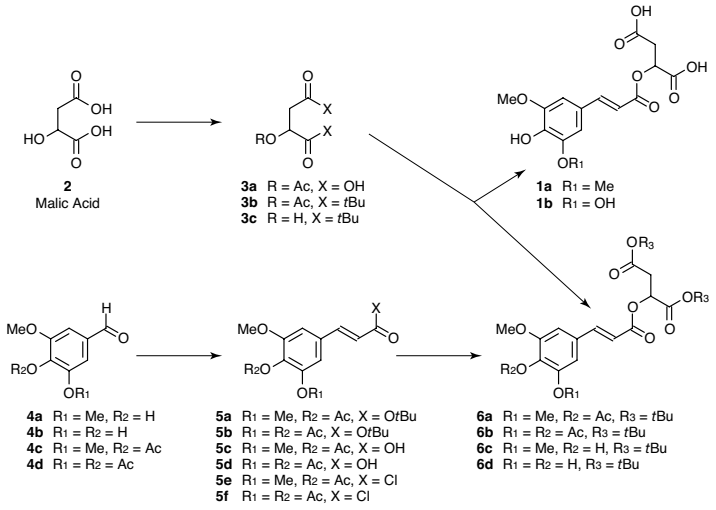

2 Malic Acid

3a R = Ac, X = OH
3b R = Ac, X = *t*Bu
3c R = H, X = *t*Bu

1a R_1 = Me
1b R_1 = OH

4a R_1 = Me, R_2 = H
4b $R_1 = R_2$ = H
4c R_1 = Me, R_2 = Ac
4d $R_1 = R_2$ = Ac

5a R_1 = Me, R_2 = Ac, X = O*t*Bu
5b $R_1 = R_2$ = Ac, X = O*t*Bu
5c R_1 = Me, R_2 = Ac, X = OH
5d $R_1 = R_2$ = Ac, X = OH
5e R_1 = Me, R_2 = Ac, X = Cl
5f $R_1 = R_2$ = Ac, X = Cl

6a R_1 = Me, R_2 = Ac, R_3 = *t*Bu
6b $R_1 = R_2$ = Ac, R_3 = *t*Bu
6c R_1 = Me, R_2 = H, R_3 = *t*Bu
6d $R_1 = R_2$ = H, R_3 = *t*Bu

Sequencing Around 5-Hydroxyconiferyl Alcohol-Derived Units in COMT-Deficient Lignins
F. Lu, J. Ralph, J.M. Marita, C, Lapierre, and W. Boerjan

Introduction

Lignins are polymeric aromatic constituents in woody plant cell walls. Although they are traditionally considered to be dehydrogenative polymers from three monolignols, *p*-coumaryl alcohol **1P**, coniferyl alcohol **1G**, and sinapyl alcohol **1S**, Fig. 1, they can vary greatly in their composition. Recently there has been considerable interest in genetically modifying lignins with the goal of improving the utilization of lignocellulosics in various agricultural and industrial processes. Studies on mutant and transgenic plants with altered monolignol biosynthesis have suggested that plants have a high level of metabolic plasticity in the formation of lignin. Lignins in angiosperm plants with depressed COMT (caffeic acid *O*-methyltransferase) were found to include significant amounts of 5-hydroxyconiferyl alcohol monomers **15H**, substituting **15H** for the traditional monomer, sinapyl alcohol **1S**. NMR analysis of lignins from poplar deficient in COMT revealed that benzodioxane structures are formed through β–O–4-coupling of a monolignol with 5-hydroxyguaiacyl unit, followed by internal trapping of the resultant quinone methide by the phenolic 5-hydroxyl. When the lignins were subjected to thioacidolysis, a novel 5-hydroxyguaiacyl monomer **2** was found in addition to the normal guaiacyl and syringyl thioacidolysis monomers. Also, a new compound **3G** was found in the dimeric products of the thioacidolysis followed by Raney nickel desulfurization, Fig. 1.

Further study with the lignins using the DFRC method also confirmed the existence of benzodioxane structures in this lignin, with compounds **4**, Fig. 1, being identified. However, the monomeric 5-hydroxyguaiacyl unit could not be detected in the DFRC products of the lignin. These facts suggested that the DFRC does not cleave the benzodioxane structures and might therefore be useful as an analytical tool for determination of benzodioxane structures linked by β–O–4 ethers. Using a modified DFRC procedure, we report here our results that provide further evidence for the existence of benzodioxane structures in lignins of COMT-deficient plants (and therefore that 5-hydroxyconiferyl alcohol is behaving as a monolignol and can be integrated into plant lignins), and demonstrate the usefulness of the DFRC method for determining the details of 5-hydroxyconiferyl alcohol incorporation into lignins.

Experimental Procedures

Materials

Two independent sets of COMT-deficient poplar lignin samples were used in this study; their lignins have been available in greater quantities than from analogously downregulated forage plants which are only now beginning to be analyzed. One is from antisense methods; the other, with even lower COMT-activity, is from sense-suppression (gene-silencing).

Compounds **5**-**6** were synthesized by methods too complex to describe here (Fig. 2).

Modified DFRC procedure for COMT-deficient lignins and cell walls

DFRC: Lignins (8 to 10 mg) or extracted wood cell wall (40 mg) were used. The acetyl bromide treatment and zinc reduction steps were performed as the standard DFRC procedure. After the zinc reduction step the degraded products were methylated as follows (instead of acetylation).

Methylation: the above residue was methylated with iodomethane (50 ml) and cesium carbonate (100 mg) in 3 ml acetonitrile for 30 min. The excess reagents were quenched by addition of 1 ml acetic acid and the product isolated.

Solid phase extraction (**SPE**): The above residue was transferred with 2 ml dichloromethane into a 10 ml pear shape flask, concentrated to less than 50 ml, and loaded with dichloromethane (the total volume should not larger than 150 ml) to a 3 ml pre-conditioned (5/1 cyclohexane/ethyl acetate) normal phase SPE column (LC-Si, Supelco). The monomers were eluted with 9 ml cyclohexane/ethyl acetate (5/1, v/v). Then the dimeric products were eluted with 9 ml cyclohexane/ethyl acetate (1/1.5, v/v). This dimeric fraction was evaporated under reduced pressure.

Hydrolysis: The above dimeric products were dissolved in 3 ml methanol in a 25 ml flask to which 3 ml 1 M potassium carbonate aqueous was added. This mixture was stirred for 1 h. The solution was concentrated to about 3 ml and acidified with 4 ml 1 M aqueous HCl solution and saturated with sodium chloride followed by extraction with dichloromethane (3x10 ml). The combined dichloromethane extracts were dried over anhydrous sodium sulfate and evaporated under reduced pressure after filtration.

TMS-derivatization and GC analysis: The above residue was transferred with 2 ml dichloromethane into a 10 ml pear shape flask and internal standard (mono-4-methylated 5–5-diferulic acid) in pyridine 10-15 ml were added. The products were concentrated and transferred into a reacti-vial with 50 ml pyridine and derivatized with 50 ml BSTFA for 30 min at 50 ˚C before 5 ml was injected into the GC.

Results and Discussion

The fact that 5-hydroxyconiferyl acetate has not been found in DFRC degradation products of COMT-deficient poplar lignin implies that all of the 5-hydroxyconiferyl alcohol monomer is incorporated into lignin as benzodioxane structures and these structures totally survive DFRC conditions (without cleavage to monomeric products). This absolute survivability has now been demonstrated with dimeric model compounds (not shown).

When a COMT-deficient polar lignin was degraded by the standard DFRC procedure, the benzodioxane marker compound **4G** was detected by GC-MS. But the absence of the corresponding **4S** raised a question whether the syringyl benzodioxane was not in this lignin or the marker compound **4S** could not get through the GC. With synthetic compound **4S**, we found that **4S** could not survive the GC conditions because of its thermo-lability, but the TMS-derivatized compounds $\mathbf{6S_F}$ and $\mathbf{6S_E}$ (Fig. 2) proved to be amenable to GC quantitative analysis. So a modified DFRC procedure was developed (Fig. 3) to determine the benzodioxane structures. First of all, the normal DFRC allows cleavage of β-ethers and leaves the benzodioxanes intact. After zinc reduction, the phenols released due to β-ether cleavage are methylated and the phenolic acetates originally from free phenols of lignins remain unaffected. So the benzodioxanes with free phenols on G/S units in lignins will be acetylated whereas and the benzodioxanes with etherified phenols on G/S units become methylated. A solid-state extraction step was used to clean up sample and enrich the dimeric products, allowing more accurate GC analysis. The final step in this procedure, base hydrolysis, converts all benzodioxane dimers in DFRC degradation products into compounds **6**. Their TMS-derivatives were analyzed by GC.

The partial FID-GC profiles of the degradation products of four samples by the modified DFRC procedure are shown in Fig. 4. The target compounds **6** were identified by mass spectra and GC retention time comparison with synthetic and authentic model compounds. An internal standard 4-monomethylated 5–5-diferulic acid was added to samples right before TMS-derivatization and GC analysis.

From the results summarized in the Table, it can be seen that guaiacyl benzodioxanes released by DFRC mostly (70-86%) were from the end of lignin molecules and the released syringyl benzodioxanes mostly (67-77%) were from lignins' internal units. By comparing results of MWL and residual lignin after dioxane extraction, some partitioning of benzodioxane structures among lignin fractions occurred during preparation of MWL with dioxane extraction and this partitioning is more significant for the guaiacyl benzodioxanes than for the syringyl ones.

One important aspect to note (that also applies to a lesser degree to the thioacidolysis products) is that the overall yields for benzodioxanes released by DFRC are relatively low compared to results obtained from NMR analysis of the lignins. Since 5-hydroxy-units could also couple with further 5-hydroxyconiferyl alcohol monomers producing benzodioxane chains that are not cleavable by DFRC, trimers, tetramers and higher oligomers of benzodioxane chains may exist in DFRC products and can not be measured by GC. In fact, evidence for such benzodioxane chains has recently been demonstrated in a COMT-deficient alfalfa transgenic. The isolation of those trimers or tetramers will give further evidence that 5-hydroxyconiferyl alcohol is truly a monolignol that is integrated into lignins, particularly of COMT-deficient plants.

Conclusion

In summary, a combination of prior NMR and thioacidolysis data and this DFRC data demonstrates compellingly that 5-hydroxyconiferyl alcohol is incorporating intimately into lignins like the traditional monolignols…

• 5-Hydroxyconiferyl alcohol is cross-coupling (at its b-position) with the phenolic end of growing lignin oligomers, and…

• New monolignols (**1G**, **1S**, and **15H**) can all cross-couple with the newly formed 5-hydroxyguaiacyl end unit, extending the chain in a typical endwise fashion, and…

• Further monolignols will cross-couple with the new end-unit from this latest addition, such that it too becomes further etherified.

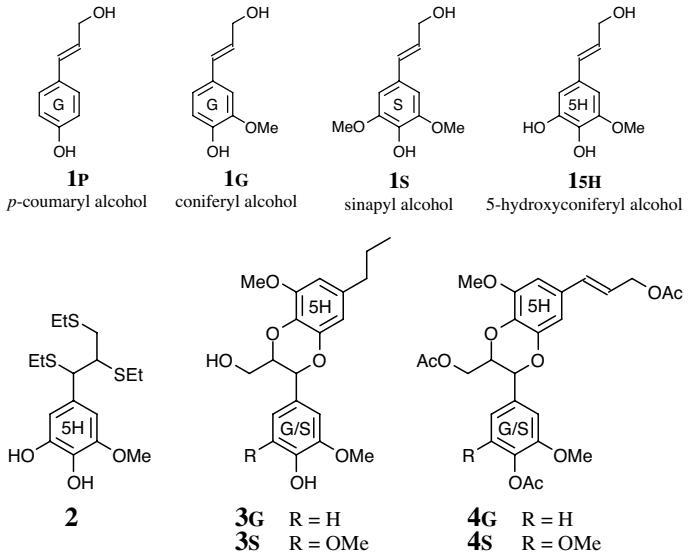

Figure 1. The monolignols **1**, and marker compounds **2**-**4** resulting from 5-hydroxyconiferyl alcohol incorporation into lignins; thioacidolysis monomeric marker **2**, dimers **3**, and DFRC dimeric markers **4**.

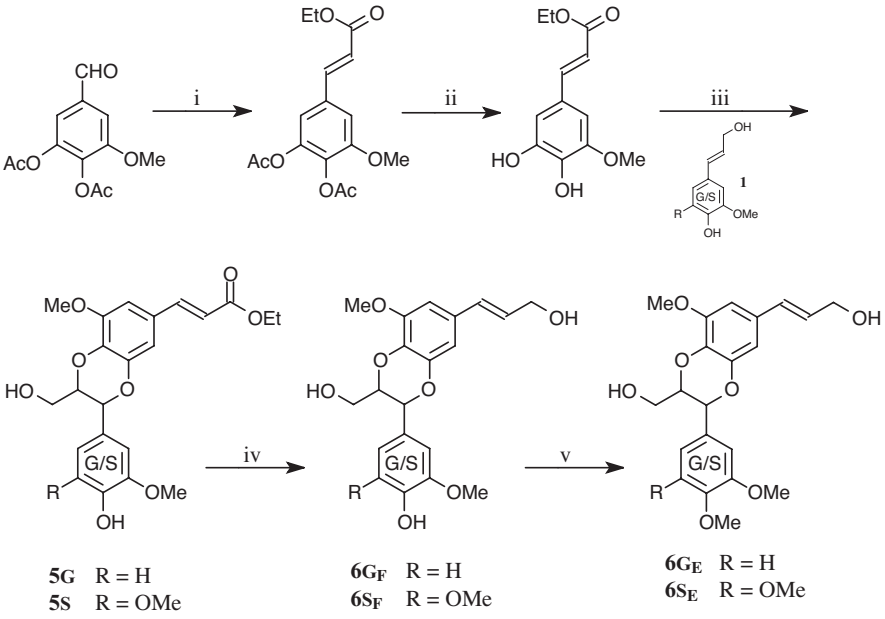

Figure 2. Synthesis of products **5**-**6** required for DFRC methods. i. NaH-triethyl phosphonoacetate,THF; ii. pyrrolidine; iii. Ag_2CO_3, benzene-acetone (5/1, v/v); iv. DIBAL-H, toluene; v. CH_3I-K_2CO_3-acetone.

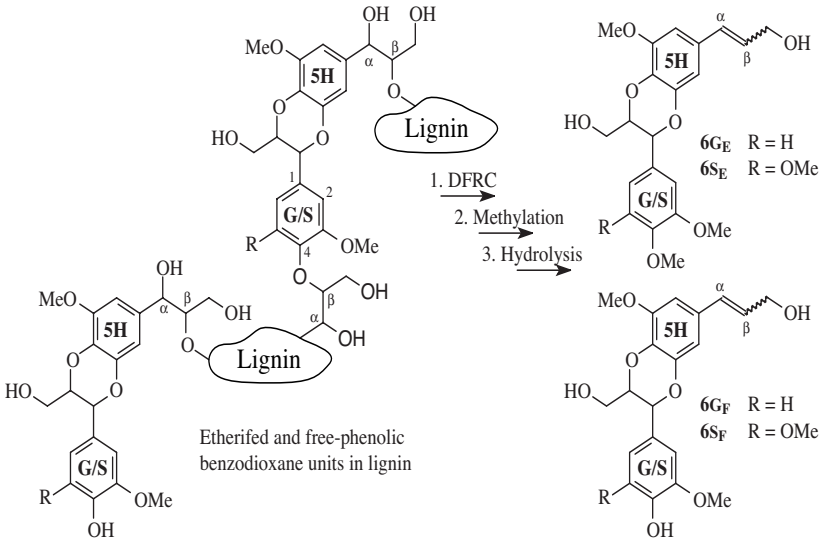

Figure 3. Benzodioxane compounds released from DFRC degradation of a hypothetical lignin containing free-phenolic and etherified benzodioxane units.

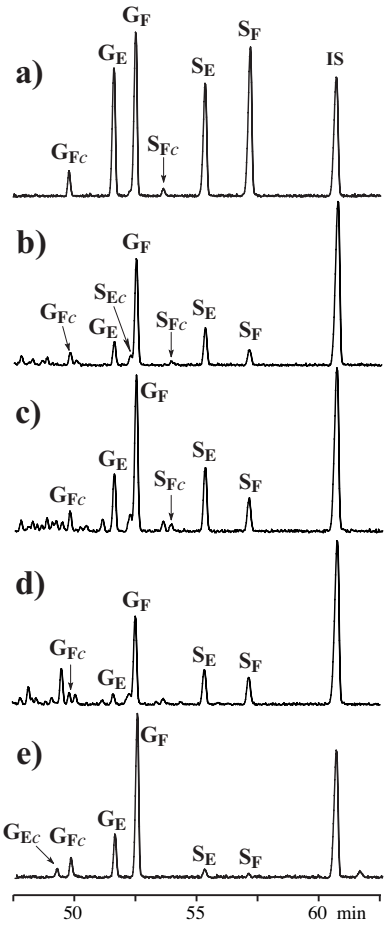

Figure 4. Partial GC-FIDs showing TMS-derivatized benzodioxane products from degradation of COMT-deficient poplar lignins or cell walls by the modified DFRCprocedure.
a) Synthesized models.
b) antisense COMT-deficient poplar lignin.
c) residual lignin after isolation of lignin in b.
d) antisense COMT-deficient poplar cell wall.
e) Gene-silenced COMT-deficient poplar lignin.

Sample Description	Relative Ratios		Overall yields (%lignin sample)		
	GOMe/GOH	SOMe/SOH			
	6GF/6SF	6GE/6SE	G (6GF+6SF)	S (6GE+6SE)	G/S
Lignin (antisense)	20/80	72/28	0.39	0.19	2.05
Residual Lignin (antisense)	30/70	71.5/28.5	--	--	1.33
Lignin (sense)	26.5/73.5	77.3/22.7	0.43	0.02*	21.5*
Cell wall (antisense)	13.5/86.5	66.7/33.3	--	--	0.93

An Improved ^{13}C-Tracer Method for the Study of Lignin Structure and Reactions — Differential 2D $^{13}C/^{1}H$-NMR

N. Terashima, D. Evtuguin, C. P. Neto, J. Parkås, M. Paulsson, U. Westermark, S. Ralph and J. Ralph

Introduction

Lignin is a structurally heterogeneous polymer formed from several kinds of monolignols by an irreversible, combinatorial radical polymerization. Therefore, it is impossible to degrade lignin quantitatively into monomeric or oligomeric units, and degradation loses information on its 3D macromolecular structure. Accordingly, destructive analyses can provide limited information on the chemical structure of protolignin in the cell wall. Among various non-destructive analytical methods, NMR spectrometry is one of the most powerful techniques that provides direct information on the structure of lignin. In the ^{13}C-NMR spectrum, signals are distributed over a wide range of chemical shifts. However, considerable overlap of the signals sometimes causes difficulty in assignments of weak signals and in quantitative determination of the signal intensities. Two-dimensional spectrometry provides a remarkable improvement in assignment and quantitative determination of the signal intensities. Nevertheless, there is still some overlapping of signals.

Selective ^{13}C-enrichment of a specific carbon in the lignin improves the signal intensity of the enriched carbon in its ^{13}C-NMR spectrum, and the difference spectrum between spectra of ^{13}C-enriched and unenriched lignins allows further improvements in the assignment of the signal and quantitative determination of the intensity. Selective ^{13}C-enrichment is achieved by feeding ^{13}C-enriched lignin biosynthesis precursors to the growing stem of a tree or inner cavity of a plant stalk. The monolignol glucosides have been shown to be the best precursors. The ^{13}C-NMR also gives information on the behavior of the bonds and functional groups during various types of reactions that is difficult to obtain by any other conventional destructive analyses.

This paper demonstrates that exceedingly clean differential spectra can be obtained by 2D NMR for synthetic lignins as a prelude to the application for isolated lignins.

Methods

Preparation of ^{13}C-labeled synthetic lignins.

Coniferins specifically ^{13}C-enriched at the side chain carbons, α, β, γ and at the aromatic ring car-

bons 1, 3, 4 and 5 were synthesized by the procedure of Terashima *et al*., and the solution of the coniferins in phosphate buffer (pH 6.0) was treated with a mixture of three kinds of enzymes, β-glucosidase, glucose oxidase and peroxidase to produce guaiacyl (G) type synthetic lignin (DHP).

Results and Discussion

For a DHP with a hypothetical structure such as shown in Fig. 1, two types of 2D ^{13}C–^{1}H partial spectra (just the sidechain regions) are shown on the left and right columns of Fig. 2. The left column (a-d) has HSQC spectra in which each carbon correlates with its directly attached carbon. The right column (e-h) shows each carbon correlating with all of the protons in the sidechain from that unit. [The spectra are much more readily interpreted in the color version of this figure which is on the CD version of these Research Summaries or on our web site at www.dfrc.wisc.edu]. The unlabeled control shows correlations from all three carbons and their associated protons, whereas the differential spectra from the specifically enriched lignins show only correlations with the enriched carbons, remarkably cleanly. Evidence for the excellent subtraction is the disappearance of the strong methoxyl group in the 2D difference spectra for Cα-Cβ. Coniferin unfortunately appears to be incorporated as an α-O-6 (glucose) ether in these DHPs.

With the labeling and NMR subtraction methods in hand, these techniques (along with a full quantitative analysis of the 1D ^{13}C NMR spectra) will be attempted for actual lignins by Terashima and colleagues.

Acknowledgements

Financial support from the research foundation Stiftelsen Nils och Dorthi Troëdssons Forskningsfond is gratefully acknowledged.

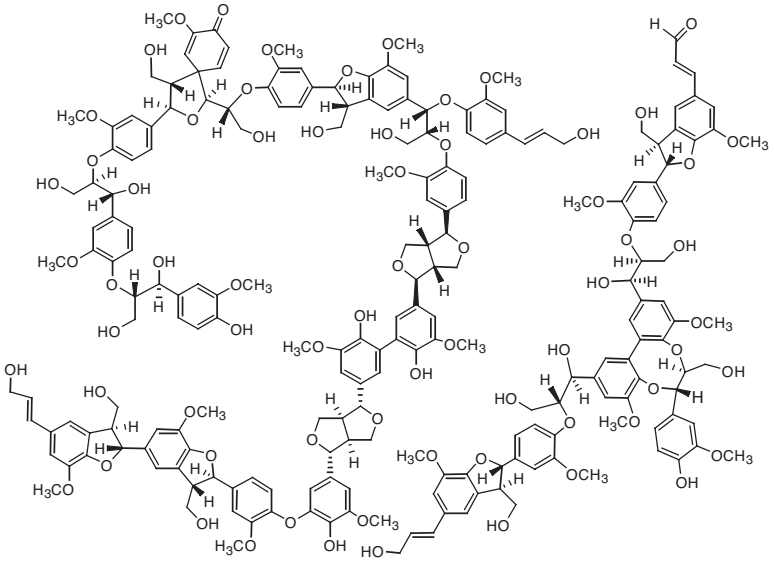

Figure 1. A part of proposed structure for the G-DHP

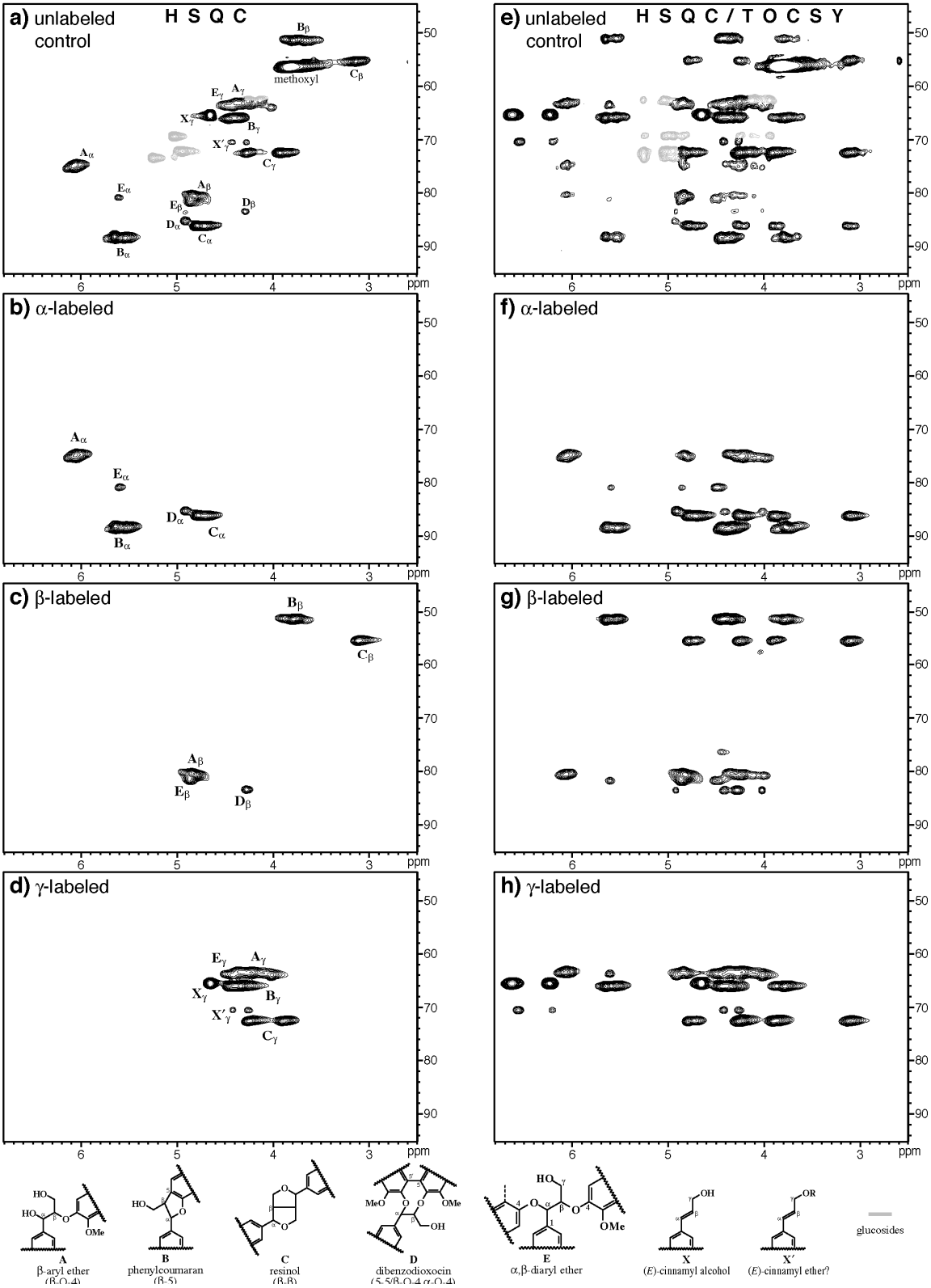

Figure 2. Two-dimensional spectra of acetates of ^{13}C-enriched DHPs. a-d) HSQC spectra. a): unenriched control. b)-d): Difference spectra obtained by subtraction of the spectrum of the unenriched control from the spectra of DHPs specifically ^{13}C-enriched at side-chain carbon, Cα, Cβ, Cα. e-f) Analogous HSQC-TOCSY spectra — see text.

Variations in the Cell Wall Composition of Maize *Brown Midrib* Mutants

J.M. Marita, W. Vermerris, J. Ralph, and R.D. Hatfield

Introduction

There are four *brown midrib* (*bm*) mutants known in maize (*Zea mays* L.). These mutants, *bm1*, *bm2*, *bm3* and *bm4*, are believed to be Mendelian recessives and recognized by reddish-brown vascular tissue in their leaves and stems. The *bm* mutants are of interest because of their potentially higher nutritional value as a forage, presumably because of the lower lignin content and more digestible cell wall structure. The data presented represented a comprehensive analysis of the effects of *bm* mutations on lignin in a single genetic background. There were variations in the *bm* mutational effects compared to results previously published in other genetic backgrounds. This may be attributed to the multiplicity of genes in maize whereby a mutational effect in one isoform is compensated for by other isoforms present and functioning or variable expression of a specific transgene having different impacts depending on the genetic background in which it is being expressed.

Results and Discussion

Nuclear Magnetic Resonance - NMR

Lignin itself is a complex polymer that hardens the cell walls of a plants xylem tissue. The *bm1* mutation has been shown to affect the activity of the enzyme cinnamyl alcohol dehydrogenase (CAD) and the Bm3 gene corresponds to an insertion and a deletion in the caffeic acid *O*-methyltransferase (COMT) gene, both involved in the lignin pathway. The *bm1* and *bm3* mutational effects (elevated aldehyde levels and the presence of benzodioxane units **H** signatures of CAD and COMT-deficiencies) were undeniably present as determined by NMR. The most striking difference discovered by NMR was the significant presence of benzodioxane units in the *bm3* isolated lignin.

Maize Cell Walls (CW)

The CWs from the *bm3* and *bm1-bm2* mutants had a 20% and 10% lower lignin content compared to wild-type, while the *bm1*, *bm2* and *bm4* mutant CWs contained the same amount (Table 1A). The *bm* mutants are generally recognized by a reduction in lignin content; however, the results from numerous studies vary to the same extent as the number of genetic stocks investigated. Consequently, differences in the lignin content of any given *bm* mutation compared to wild-type were quite variable.

The sum of Klason lignins, total neutral sugars and uronic acids accounted for 92% to 95% of the *bm* mutant cell wall. The proportion of individual neutral sugars (mg g^{-1} CW) was generally the same for all CWs; between 47 to 50% cellulose (as determined by glucose) and 22 to 27% xylan (as determined by xylose) with substitution with arabinose varying between 1:8 in the *bm3* mutant and 1:6 in wild-type maize.

The most noticeable changes in cell wall composition were elevated levels of ferulate (FA) monomers in the *bm3* mutant with no change in the amount of cross-linking (as evidenced from etherified-FA levels; Table 2). The only maize samples to show a reduction in their level of cross-linking (between arabinoxylans indicated by total FA dimers) were the *bm1* and *bm1-bm2* mutants. Any attributable mutational effects in the *bm1-bm2* CWs appear to be *bm1* in origin, especially changes in cell wall composition; however, since exact *bm2* mutational effects are not known, other param-

eters than those examined may represent more closely the *bm2* mutational effect. Esterified-*p*Coumarate (pCA) levels were variable among all maize samples with the *bm1*, *bm3* and the double *bm1-bm2* mutants having ~50% less esterified-*p*CA than all other CW maize samples.

Maize Lignin Extract (LE) and Lignin Residue (LR) Fractions
Striking differences between the *bm* mutants were revealed by compositional shifts in their LR and LE fractions. When enzyme digested cell walls are partitioned into the LE and LR fractions, the sum of their Klason lignin values should theoretically add up to the corresponding CW Klason lignin value. However, the sum for all samples, particularly the *bm* mutants, was lower. Differences in the levels of acid soluble components lost during hydrolysis and/or differences in individual carbohydrate profiles may account for such discrepancies.

Parallel reductions in esterified-*p*CA were observed in the same maize LR and LE fractions; every maize sample had lower total esterified-*p*CA (LR+LE) than amounts released from their CW. For example, the *bm1* mutant displayed the greatest reduction at 46% of its CW level (68% of the wild-type level). This parallels the reduction observed in the *bm1* mutant Klason lignin (LR+LE) at 53% of its CW level (51% of the wild-type level).

Previous reports suggested that little *p*CA is esterified to arabinoxylans in maize; therefore, the *p*CA released during low temperature hydrolysis must be predominantly esterified to lignin in the LR and LE fractions. These results suggest that *p*CA-lignin complexes were solubilized and lost in the supernatants during cellulase enzyme treatment. Low temperature alkaline hydrolysis of the enzyme supernatants did reveal substantial amounts of esterified-*p*CA. Furthermore, 0.1 N trifluoroacetic acid (TFA) hydrolysis of the maize CWs released *p*CA-arabinosyl-conjugates, detectable by GC/MS selective ion monitoring. Since only small amounts of *p*CA were found esterified to arabinoxylans in the maize samples, the esterified-*p*CA measured after low temperature hydrolysis from the supernatants clearly indicates that significant amounts of *p*CA-lignin complexes are being solubilized during cellulase enzyme treatment. These results help explain why parallel reductions of *p*CA and lignin were observed in the *bm* mutant LR and LE fractions; specifically, the higher the solubility of *p*CA-lignin complexes in the *bm* mutants, the greater the loss after the cellulase enzyme treatment.

Compositional shifts in total neutral sugars existed between the LR and LE fractions, Table 1B. Cellulose (as measured by glucose) was greater in all the maize LR fractions versus LE fractions. The *bm3* mutant with the greatest degradability (88%) had the lowest residual cellulose (LR+LE glucose; 40 mg g^{-1} CW), whereas the *bm4* mutant with the lowest degradability (71%) had the highest residual cellulose (LR+LE glucose; 134 mg g^{-1} CW). Individual neutral sugars were not partitioned equally among samples implying that the hydrolysis of component polysaccharides was not consistent across *bm* mutants. Equivalent neutral sugars levels (mg g^{-1} CW) were observed among the maize LE fractions suggesting that the composition of the neutral sugars extracted in the soluble lignin fraction among all maize samples is the same regardless of the *bm* mutation. The presence and detection of neutral sugars in the LE fraction supports an interaction between carbohydrates and lignin. A reasonable conclusion since arabinoxylans are known to be cross-linked to lignin by FA.

The reason why neutral sugar components are partitioned predominantly into the LR fraction may be an organizational issue whereby their incorporation into the cell wall is dependent on the respective *bm* mutation being expressed. Other studies of *bm* maize have alluded to these plants lacking some

function controlling lignification. These data would suggest that the function lacking does not control lignification *per se* but may control *elements* leading to lignification such as peroxidase activity or hydrogen peroxide production availability. As a result, the lignin polymer is altered in such a way that incorporation of esterified-*p*CA is reduced and consequently the structure of the lignin polymer altered at some organizational ("non-polymeric") level not detected. Because of a difference in the structural organization of lignin there is less *p*CA incorporation and greater solubility of smaller-sized *p*CA-lignin complexes. Further study into greater solubility versus greater degradability should be of interest.

Experimental Procedures

Lignin isolation and preparation

The stalk sections were cut into 2-3 cm pieces and ground to pass a 2.0 mm screen of a Wiley mill prior to a cyclone mill (1 mm). The ground maize stems were extensively extracted with water, methanol, acetone, and chloroform. The isolated CW's were ball-milled, digested with crude cellulases, and extracted into 96:4 dioxane:H_2O. The dioxane:water fractions were lyophilized and saved as maize lignin extract (LE) and maize lignin residue (LR).

Cell Wall Composition

For all CW, LR, and LE samples, Klason lignin, total uronic acids, total neutral sugars, and phenolic compositions were determined. Klason lignin determinations were the ash-corrected residue remaining after total hydrolysis of CW polysaccharides. Total uronic acids were estimated colorimetrically with glacturonic acid as the calibration standard. Neutral sugars from total CW hydrolysis were determined by high-pressure liquid chromatography. CW (~50 mg), LR (~55 mg), and LE (~30 mg) samples were analyzed for esters and ethers using internal standards, 2-hydroxycinnamic acid (0.1 mg) for monomers and 5-5-diferulic acid monomethyl ether (0.05 mg) for dimers. Derivatives of phenolic acids were separated by gas liquid chromatography.

Table 1A. Cell wall (CW) composition of wild-type and *bm* mutants of maize in A619 background averaged over two replicates. **B.** The sum of dioxane:H_2O residue (LR) and dioxane:H_2O extract (LE) total neutral sugars (TNS) of wild-type and *bm* mutants of maize in A619 background and percent cell wall digested following cellulase enzyme treatment (averaged over two replicates).

A	**A619**	***bm1***	***bm2***	***bm3***	***bm4***	***bm1-bm2***
Klason lignin (mg g^{-1} CW)	130±3	130[a]	131±4	104±2	138±1	118±3
Uronosyls (mg g^{-1} CW)	41±2	49±2	43±2	37±0	41±2	42±0
TNS (mg g^{-1} CW)						
Arabinose	36.7±0.6	34.4±0.1	32.6±0.3	32.7±1.0	34.4±0.6	33.0±0.5
Glucose	479.1v±5.4	471.8±20.3	469.1±4.2	491.2±3.5	485.7±7.1	472.5±9.7
Xylose	226.6±3.2	252.9±0.4	252.0±4.9	262.1±3.2	242.0±0.3	244.9±3.9
Total[b]	755.4	770.1	764.6	796.5	772.2	761.2
Cell Wall Total[c]	927	949	939	937	951	920
B						
TNS – LR (mg g^{-1} CW)						
Arabinose	6.6±0.0	5.0±0.1	6.4±0.0	2.3±0.1	7.4±0.5	5.0±0.0
Glucose	62.4±11.4	67.9±2.9	91.4±1.3	38.0±0.7	131.2±5.4	66.7±1.4
Xylose	56.8±1.0	60.4±2.8	71.5±0.7	26.3±0.9	89.4±4.4	50.2±0.2
Totals[b]	129.4	135.2	171.3	68.0	230.7	124.7
TNS – LE (mg g^{-1} CW)						
Arabinose	1.6±0.1	0.9±0.0	1.4±0.0	1.5±0.0	1.3±0.1	1.1±0.0
Glucose	5.4±0.3	1.9±0.0	2.9±0.2	1.9±0.0	2.9±0.2	4.4±0.1
Xylose	14.0±0.0	8.3±0.1	11.9±1.0	10.8±0.5	10.9±0.6	8.8±0.1
Totals	21.2	11.3	16.3	14.2	15.3	14.4
% degradability[d]	76%	82%	77%	88%	71%	82%

[a] Based on one replicate
[b] Total =∑(fucose+arabinose+rhamnose+galactose+glucose+xylose+mannose)
[c] Cell Wall Total =∑(Klason Lignin+Uronosyls+Total Neutral Sugars)
[d] Degradability is ((1-recovered weight/initial weight) mg g^{-1} CW)

Table 2 Cell wall (CW) phenolic acids released from wild-type and *bm* mutants of maize in A619 background averaged over two replicates.

	A619	*bm1*	*bm2*	*bm3*	*bm4*	*bm1-bi*
Monomers(mg g^{-1} CW)						
esterified-*p*CA	14.07±0.20	8.46±0.02	15.03±0.18	7.90±0.10	16.14±0.03	7.89±0.24
esterified-FA	4.46±0.07	5.09±0.05	5.24±0.24	7.29±0.07	4.67±0.09	4.89±0.01
etherified-FA	2.21±0.05	1.85±0.19	2.69±0.24	2.51±0.23	2.36±0.11	1.78±0.19
% wild-type	100%	84%	122%	114%	107%	81%
FA dimers(mg g^{-1} CW)						
Dimer total	1.85	1.96	1.79	1.87	1.90	1.50
FA Total	8.52	8.90	9.72	11.67	8.93	8.17

Modifications in Lignin of Transgenic Alfalfa Down-Regulated in COMT and CCoAOMT

J.M. Marita, J. Ralph, R.D. Hatfield, D. Guo, F. Chen, R.A. Dixon

Introduction

Alfalfa (Medicago sativa L.) is a leading forage crop. It has high nutritive value because it is rich in protein, minerals, and vitamins, and if harvested prior to flowering can retain a low fiber and high energy content. The intake and digestibility of forage by dairy animals directly affect their production of meat and milk. A reduction in feeding value results from a lower leaf to stem ratio and the deposition of lignin and polysaccharides in stem cell walls during maturation. The present study examined the alterations to alfalfa lignin structure and composition resulting from independent down-regulation of caffeic acid 3-O-methyltransferase (COMT) and caffeoyl Coenzyme A 3-O-methyltransferase (CCoAOMT) two key enzymes in the lignin pathway. Previous work has shown genetically modified alfalfa to have altered lignin composition and improved in situ digestibility. The results of this study reveal new details of the incorporation of novel units in the lignin of COMT-deficient alfalfa including units not previously identified and an increase in the cellulose:lignin ratio in CCoAOMT-deficient alfalfa. This information allows researchers insight into which lignin structural modifications positively impact alfalfa digestibility.

Results and Discussion

COMT-deficient alfalfa

2D NMR experiments allowed structural analysis of the major units in isolated lignin from alfalfa. Quantification of interunit type structures based on measuring volume integrals in the 2D HMQC spectra (8) of wild-type and COMT-deficient alfalfa are presented in Table 1.

Table 1. Subunit ratios derived from volume integrals of contours in $^{13}C–^{1}H$ correlation spectra of alfalfa lignin.

Alfalfa Lignin	Unit Type, Relative Proportion						
	A	**B**	**C**	**D**	**H**	**X**	**Σ(β-ethers)[a]**
Wild-type	81	8	6	1	0	3	83
COMT	44	8	3	4	38	4	85
CCoAOMT	88	5	6	0	<1	2	88

[a] Σ(β-ethers) = **A**+**D**+**H**

A=β-O-4; **B**=β-5; **C**=β-β; **D**=5-5/β-O-4/α-O-4; **H**=benzodioxanes; **X**=cinnamyl alcohol endgroups

Most striking was the presence of novel benzodioxane units **H** (38%) in the COMT-deficient alfalfa at the levels of the normal β-ether units **A** (44%). In the wild-type alfalfa, no benzodioxane units **H** were detected; the lignin was comprised of mainly β-ether units **A** (81%).

Long-range correlation spectra provided valuable insight into which types of units were connected to each other. Specifically, HMBC data revealed the extent of S/G compositional changes in β-aryl ether units **A** in the extractable isolated lignins. The correlations clearly showed that the lignin was significantly syringyl depleted. HMBC spectra, also indicated the presence of new 5-hydroxyguaiacyl-glycerol structures $\mathbf{G_{5H}}$ (Fig. 1). Although glycerol structures are typically rare in lignins, they are clearly unique to the 5-hydroxyguaiacyl units in the COMT-deficient alfalfa. HMBC experiments provided compelling evidence that 5-hydroxyconiferyl alcohol was incorporated intimately into the polymerization process. In the examined isolated lignin, the HMBC spectrum showed that about half of the 5-hydroxyguaicyl units were etherified (into benzodioxane structures) by reacting with coniferyl alcohol monomers and about half by reacting with another 5-hydroxyconiferyl alcohol monomer. The 5-hydroxyconiferyl alcohol $\mathbf{1_{5H}}$ was participating in endwise coupling reactions extending the lignin chain in an analogous manner to the normal monolignols, coniferyl alcohol $\mathbf{1_G}$ and sinapyl alcohol $\mathbf{1_S}$ (Fig. 2). Therefore, it is logical to consider 5-hydroxyconiferyl alcohol as an authentic monolignol in these COMT-deficient transgenics,. These observations strongly support our contention that a non-traditional monomer can be utilized for lignification when biosynthesis of traditional monolignols is interrupted.

Klason lignin and total neutral sugars were determined. COMT-deficient alfalfa resulted in a 10% decrease in Klason lignin content compared to wild-type. This decrease in lignin content, was complimented by a (relative) increase (~10%) in cellulose (as measured by glucose) and an increase (~6%) in xylans (as measured by xylose). Alfalfa leaves provide the most nutrition to the animal and stems a limiting component. Any increase in availability of nutrients tied up in the stem should positively affect the overall benefit of the forage to the animal. Off-site examination of rumen digestibility of alfalfa forage in fistulated steers revealed just that — improved digestibility of forage from COMT down-regulated alfalfa plant.

CCoAOMT-deficient alfalfa

Similar structural and compositional analyses were done on isolated lignin from CCoAOMT-deficient alfalfa. All major structural units were still present in the lignin of the CCoAOMT-deficient alfalfa at similar intensities to wild-type levels (Table 1). The only structural and compositional differences were detected near baseplane levels where **H** (benzodioxane) units became discernable.

Klason lignin and total neutral sugars were also determined. The CCoAOMT-deficient alfalfa re-

sulted in a 21% decrease in lignin content compared to wild-type. Unlike the COMT-deficient alfalfa, the complimentary (relative) increase (~11%) in cellulose (as measured by glucose) and increase (~9%) in xylans (as measured by xylose) were not equivalent to the reduction in lignin content. This corresponded to a 39% increase in cellulose:lignin ratio compared to wild-type. The decrease in *in situ* digestibility reported for CCoAOMT-deficient alfalfa is likely a consequence of the CCoAOMT transgenic cell wall attributes, particularly the polysaccharide:lignin ratio.

In general, COMT deficiency resulted in the incorporation of novel units undetected in the normal wild-type, because the plant apparently utilizes monomers from incomplete monolignol synthesis to augment the production of lignin. It appears that COMT-deficiency in legumes such as alfalfa leads to similar compositional changes as COMT-deficiency in hardwoods such as poplar. The extent of these changes varies but the signature effects are clearly evident. For the first time, there is evidence that the next reaction in the lignification sequence following incorporation of 5-hydroxyconiferyl alcohol can be the coupling with either coniferyl alcohol (or sinapyl alcohol) or another 5-hydroxyconiferyl alcohol monomer. The compositional changes evident in the CCoAOMT-deficient alfalfa potentially enhance the utilization of alfalfa as a major forage crop by increasing the digestibility of its normally poorly digestible stem fraction. The data also further support the bi-functional role of CCoAOMT in the lignin pathway and the possible interactions between the two *O*-methyltransferases, CCoAOMT and COMT.

Experimental Procedures

Lignin isolation and preparation

Stem sections were ground to pass a 1.0 mm screen of a cyclone mill. The ground stems were extensively extracted with water, methanol, acetone, and chloroform. The isolated CWs were ball-milled, digested with crude cellulases, and extracted into 96:4 dioxane:H_2O. The soluble dioxane:water fractions were lyophilized before they were dissolved in ~400 μL acetone-d_6 for NMR analysis.

Cell Wall Composition

Klason lignin determinations were the ash-corrected residue remaining after total hydrolysis of CW polysaccharides. Total uronic acids were estimated colorimetrically with glacturonic acid as the calibration standard. Neutral sugars from total CW hydrolysis were determined by HPLC.

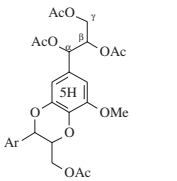

5-hydroxyguaiacyl glycerol structures

G_{5H}

Figure 1. 5-Hydoxyguaiacyl units with an acetylated glycerol sidechain.

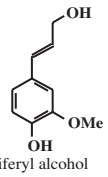

coniferyl alcohol

1_G

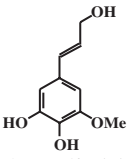

5-hydroxyconiferyl alcohol

1_{5H}

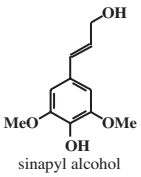

sinapyl alcohol

1_S

Figure 2**.** Resulting lignin precursors in the lignin biosynthetic pathway in angiosperms.